Electronic Supplementary Information

Biomimetic engineering of metal-organic framework on single-chiral-site precision for asymmetric hydrogenation

Jun Guo,*[a,b] Yulong Duan,[a] Yangyang Liu,[c] Huangxu Li,[d] Yin Zhang,[b] Chang Long,[b] Zuming Wang,[e] Yongchao Yang,[c] and Shenlong Zhao*[c]

[a] State Key Laboratory of Separation Membranes and Membrane Processes, School of Chemistry, Tiangong University, Tianjin 300387, China.

[b] CAS Key Laboratory of Nanosystem and Hierarchical Fabrication, CAS Center for Excellence in Nanoscience, National Center for Nanoscience and Technology, Beijing 100190, China.

[c] School of Chemical and Biomolecular Engineering, The University of Sydney, Sydney, New South Wales, Australia.

[d] Department of Chemistry, City University of Hong Kong, Kowloon, Hong Kong 999077, China.

[e] State Key Laboratory of Biochemical Engineering, Institute of Process Engineering, Chinese Academy of Sciences, Beijing 100190, China.

* Email: junguo@tiangong.edu.cn, shenlong.zhao@sydney.edu.au

Contents

Part S1. Chemicals and Reagents

Zinc acetate anhydrous (Zn(CH$_3$COO)$_2$, 99.9%), sodium borohydride (NaBH$_4$, 98%), 4-pydidinecarboxaldehyde (97%), chloroplatinic acid hexahydrate (H$_2$PtCl$_6$·6H$_2$O, 99.95%), ethyl pyruvate (EP, 98%), D$_2$O (99.95%) and Pt on activated carbon (Pt/C, 10 wt.%) were purchased from Alfa Aesar. *l*-valine (99%), *d*-valine (98%), *l*-threonine (99%), *d*-threonine (98%), *l*-serine (99%) and *d*-serine (98%) were bought from J&K. Authorized *l*-ethyl lactate (≥99.0%) and *d*-ethyl lactate (≥99.0%) were purchased from Sigma Aldrich. Hydrochloric acid (HCl, 37 wt%), sodium hydroxide (NaOH, analytical grade), methanol (MeOH, analytical grade), ethanol (EtOH, analytical grade), isopropanol (*i*-PrOH, analytical grade), toluene (analytical grade) and glycol (analytical grade) were supplied by Beijing Chemical Reagent Company (China). The deionized water used in our experiments was obtained from the Milli-Q System. All the chemicals were used as received without further purification.

Part S2. Synthesis Methods

The synthesis of *N*-(4-Pyridylmethyl)-l-valine·HCl (*l*-Lval). The *l*-Lval ligand was synthesized according to a modified literature method.[1] Namely, 10 mL 4-pydidinecarboxaldehyde methanolic solution was slowly added into 10 mL aqueous mixture of *l*-valine (1.99 g, 17.0 mmol) and NaOH (0.68 g, 17.0 mmol). The resultant solution was stirred for 12 h at room temperature and then became dark yellow. After cooling with an ice bath, 10 mL of freshly prepared $NaBH_4$ (0.76 g, 20.4 mmol) was injected quickly and stirred for 4 h. The colorless solution was acidized to pH of 5.5 with hydrochloric acid and stirred for an additional 2 h. Then the mixture was evaporated to dryness and the product was extracted with 150 mL hot and dry ethanol 3 times. Lastly, the collected filtrates were evaporated to get pure white powder. Yield: 2.70 g, 64.9%. ^{1}H-NMR (D_2O, ppm): $-CH_3$ (0.98, d, 3H), $-CH_3$ (1.04, d, 3H), -CH (2.24, m,1H), -HN-CH (3.48, m, 1H), $-CH_2$ (4.31, dd, 2H), py-H (7.57, d, 2H), py-H (8.62, d, 2H). IR (KBr, cm^{-1}): $v_{as(CO2)}$, 1593; $v_{s(CO2)}$, 1563. Corresponding IR plots are available in Figure S1.

The Synthesis of *N*-(4-Pyridylmethyl)-*d*-valine·HCl (*d*-Lval) was prepared by the same method of *l*-Lval besides replacing *d*-valine with *l*-valine. Yield: 2.83 g, 68.0%. ^{1}H-NMR (D_2O, ppm): $-CH_3$ (0.98, d, 3H), $-CH_3$ (1.04, d, 3H), -CH (2.23, m,1H), -HN-CH (3.46, m, 1H), $-CH_2$ (4.29, dd, 2H), py-H (7.54, d, 2H), py-H (8.61, d, 2H). IR (KBr, cm^{-1}): $v_{as(CO2)}$, 1592; $v_{s(CO2)}$, 1563. Corresponding IR plots are available in Figure S1.

The synthesis of *N*-(4-Pyridylmethyl)-L-serine·HCl (*l*-Lser). Similarly, *l*-Lser was prepared by slowly adding10 mL 4-pydidinecarboxaldehyde methanolic solution into 10 mL aqueous mixture of *l*-serine (1.79 g, 17.0 mmol) and NaOH (0.68 g, 17.0 mmol). The resultant solution was stirred for 12 h at room temperature and became dark yellow. After cooling with an ice bath, 10 mL of freshly prepared $NaBH_4$ (0.76 g, 20.4 mmol) was injected quickly and stirred for 4 h. The colorless solution was acidized to pH of 5.5 with hydrochloric acid and stirred for an additional 2 h. Then the mixture was

evaporated to dryness and the product was extracted with 150 mL hot and dry ethanol 3 times. Lastly, the collected filtrates were evaporated to get pure white powder. Yield: 2.12 g, 53.5%. ^{1}H-NMR (D$_2$O, ppm): -HN−CH (3.71, m, 1H), -CH$_2$-OH (3.94, dd, 2H), -CH$_2$ (4.30, s, 2H), py-H (7.50, d, 2H),py-H (8.54, d, 2H).IR(KBr, cm^{-1}): ν_{OH}, 3234; $\nu_{as(CO2)}$, 1602; $\nu_{s(CO2)}$, 1564. Corresponding IR plots are available in Figure S2.

The Synthesis of *N*-(4-Pyridylmethyl)-*d*-serine·HCl (*d*-Lser) was prepared by the same method of (*l*-Lser) besides replacing *d*-serine with *l*-serine. Yield: 1.98 g, 50.2%. ^{1}H-NMR (D$_2$O, ppm): ^{1}H-NMR (D$_2$O, ppm): -HN−CH (3.73, m, 1H), -CH$_2$-OH (3.96, dd, 2H), -CH$_2$ (4.32, s, 2H), py-H (7.52, d, 2H),py-H (8.57, d, 2H). IR (KBr, cm^{-1}): ν_{OH}, 3234; $\nu_{as(CO2)}$, 1563; $\nu_{s(CO2)}$, 1564. Corresponding IR plots are available in Figure S2.

The synthesis of *N*-(4-Pyridylmethyl)-*l*-threonine·HCl (*l*-Lthr). Similarly, N-(4-Pyridylmethyl)-*l*-threonine·HCl (*l*-Lthr) was prepared by slowly adding10 mL 4-pydidinecarboxaldehyde methanolic solution into 10 mL aqueous mixture of L-serine (2.02 g, 17.0 mmol) and NaOH (0.68 g, 17.0 mmol). The resultant solution was stirred for 12 h at room temperature and became dark yellow. After cooling with ice bath, 10 mL of freshly prepared NaBH$_4$ (0.76 g, 20.4 mmol) was injected quickly and stirred for 4 h. The colorless solution was acidized to pH of 5.5 with hydrochloric acid and stirred for an additional 2 h. Then the mixture was evaporated to dryness and the product was extracted with 150 mL hot and dry ethanol 3 times. Lastly, the collected filtrates were evaporated to get pure white powder. Yield: 2.14 g, 60,0%. ^{1}H-NMR (D$_2$O, ppm): -CH$_3$ (1.21, d, 3H), -HN−CH (3.28, m, 1H), -CH$_2$ (4.11 dd, 2H), py-H (7.47, d, 2H), py-H (8.52, d, 2H).IR (KBr, cm^{-1}): ν_{OH}, 3175; $\nu_{as(CO2)}$, 1598; $\nu_{s(CO2)}$, 1564. Corresponding IR plots are available in Figure S3.

N-(4-Pyridylmethyl)-*d*-threonine·HCl (*d*-Lthr) was prepared by the same method of (*l*-Lthr) besides replacing *d*-threonine with *l*-threonine. Yield: 2.30 g, 64,5%. ^{1}H-NMR (D$_2$O, ppm): -CH$_3$ (1.20, d, 3H), -HN−CH (3.29, m, 1H), -CH$_2$ (4.12 dd, 2H), py-H

(7.49, d, 2H),py-H (8.54, d, 2H).IR(KBr, cm^{-1}): ν_{OH}, 3175; $\nu_{as(CO2)}$, 1598; $\nu_{s(CO2)}$, 1564. Corresponding IR plots are available in Figure S3.

The synthesis of *l*(*d*)-Val-MOFs. *l*(*d*)-Val-MOFs were synthesized by the previously reported method.[2] In specification, *l*(*d*)-Lval (41.6 mg, 0.2 mmol) and Zn(CH$_3$COO)$_2$·2H$_2$O (22.0 mg, 0.1 mmol) were dissolved into 5.0 mL H$_2$O. The mixture was treated under ultrasonication for 10 min. Then, the resultant clear and colorless solution was transferred into a 12 mL sealed vial and heated at a 90°C oil bath under magnetic stirring (600 rpm) for an additional 12 h. The obtained white product was isolated by centrifugation at 5000 rpm for 5 min and washed with methanol for 3 times. Finally, the white precipitates were dried at 90°C vacuum oven overnight for further characterizations and uses. *l*-Val-MOFs, IR(KBr, cm^{-1}): ν_{NH}, 3265; $\nu_{as(CO2)}$, 1608; $\nu_{s(CO2)}$, 1560; *d*-Val-MOFs, IR(KBr, cm^{-1}): ν_{NH}, 3267; $\nu_{as(CO2)}$, 1608; $\nu_{s(CO2)}$, 1559. Corresponding IR plots are available in Figure S1. Corresponding IR plots are available in Figure S1.

The synthesis of *l*(*d*)-Ser-MOFs. *l*(*d*)-Ser-MOFs were synthesized by using a mixed solvent protocol with an appropriate ratio. In details, *l*(*d*)-Lser (39.2 mg, 0.2 mmol) was dissolved into 4.5 mL H$_2$O and then mixed with 0.5 ml methanolic solution containing Zn(CH$_3$COO)$_2$·2H$_2$O (22.0 mg, 0.1 mmol). The resultant mixture was treated under ultrasonication for 10 min. Subsequently, the clear and colorless solution was heated at a 60°C oil bath under magnetic stirring (600 rpm) for an additional 6h. The obtained white product was isolated by centrifugation at 5000 rpm for 5 min and washed with methanol for 3 times. Finally, the white precipitates were dried at 90°C vacuum oven overnight for further characterizations and uses. *l*-Ser-MOFs, IR(KBr, cm^{-1}): ν_{OH}, 3475; ν_{NH}, 3267 ; $\nu_{as(CO2)}$, 1602; $\nu_{s(CO2)}$, 1562; *d*-Ser-MOFs, IR(KBr, cm^{-1}): ν_{OH}, 3482; ν_{NH}, 3267 ; $\nu_{as(CO2)}$, 1602; $\nu_{s(CO2)}$, 1560. Corresponding IR plots are available in Figure S2.

The synthesis of *l*(*d*)-Thr-MOFs. *l*(*d*)-Thr-MOFs were synthesized also by using a

mixed solvent protocol with an appropriate ratio. In details, $l(d)$-Lthr (42.0 mg, 0.2 mmol) was dissolved into 4.0 mL H_2O and then mixed with 1.0 ml methanolic solution containing $Zn(CH_3COO)_2 \cdot 2H_2O$ (22.0 mg, 0.1 mmol). The mixture was treated under ultrasonication for 10 min. Subsequently, the clear and colorless solution was heated at a 60°C oil bath under magnetic stirring (600 rpm) for 6h. The obtained white product was isolated by centrifugation at 5000 rpm for 5 min and washed with methanol for 3 times. Finally, the white precipitate was dried at 90°C vacuum oven overnight for further characterizations and uses. l-Thr-MOFs, IR (KBr, cm^{-1}): ν_{OH}, 3445; ν_{NH}, 3247 ; $\nu_{as(CO2)}$, 1599; $\nu_{s(CO2)}$, 1560; d-Thr-MOFs, IR(KBr, cm^{-1}): ν_{OH}, 3445; ν_{NH}, 3243 ; $\nu_{as(CO2)}$, 1599; $\nu_{s(CO2)}$, 1560. Corresponding IR plots are available in Figure S3.

The synthesis of Pt NPs. Pt NPs were synthesized by an established method from literature.[3] Typically, NaOH (0.50 g, 12.5 mM) and $H_2PtCl_6 \cdot 6H_2O$ (0.50 g, 0.96 mmol) were added into 50 mL glycol.[4] The mixture was stirred for 30 min to obtain a transparent yellow glycol solution and then transferred into a three-neck flask equipped with a condenser. Under the argon atmosphere, the solution was heated at 160°C with stirring for 3 h to produce dark brown Pt NPs. The products were precipitated by adding 12.5 mL of 1 M HCl and centrifugated at 8000 rpm for 10 min. And final precipitate was redispersed in ethanol for further use.

The synthesis of Pt-CMOFs supported catalysts. 25 mg of the synthesized CMOFs namely $l(d)$-Val-MOFs, $l(d)$-Ser-MOFs, or $l(d)$-Thr-MOFs was dispersed into 5 mL ethanol, and then 0.5 mL of Pt NPs solution was dropped slowly under vigorous stirring. The resultant mixture was stirred for another 2 h and isolated by centrifugation at 4000 rpm for 5 min. The precipitate was washed with ethanol 2 times to discard the residual free Pt NPs and dried at 60°C vacuum oven overnight to offer the final supported Pt-$l(d)$-Val-MOFs (1.2 wt% Pt), Pt-$l(d)$-Ser-MOFs (1.8 wt% Pt), or Pt-$l(d)$-Thr-MOFs (1.9 wt% Pt) catalyst, respectively. The absolute Pt amount among each catalyst was measured by ICP-MS.

Part S3. Catalysis and Characterizations

Asymmetric hydrogenation of EP. Catalysts including Pt-*l*(*d*)-Val-MOFs (1.2 wt% Pt), Pt-*l*(*d*)-Ser-MOFs (1.8 wt% Pt), Pt-*l*(*d*)-Thr-MOFs (1.9 wt% Pt) and commercial Pt/C with Lthr as chiral ligands were tested for systematical comparison. In a standard procedure, each catalyst with the same absolute Pt amount (1.3 μmol) was dispersed in 2 mL ethanol and then mixed with EP (10 μL). Subsequently, the mixture was transferred into a Teflon-lined stainless steel autoclave and was purged with H_2 three times. Finally, the hydrogen pressure of the autoclave was set at 4 MPa and the reaction was magnetically stirred at 25°C for 12 h. The obtained filtrate was collected by centrifugation and analyzed by chiral gas chromatography (GC, GC-2010 Plus, Shimadzu) installed with flame ionization detector and HP19091G-B213 capillary column (30 m×0.32 mm×0.25 um). The optical yield of the product was expressed as ee value: ee (%) =([R]-[S])/([R]+[S])×100 and the absolute configuration of the product was confirmed by authorized enantiomer available from commerce. To use ^{1}H-NMR to characterize the produced ethyl lactate qualitatively, deuterated CD_3OD was replaced with CH_3OH as the solvent under otherwise same conditions to standard procedures. After filtration of the heterogeneous catalyst, the produced ethyl lactate dissolved into CD3OD was taken for ^{1}H-NMR testing.

Characterizations. Transmission electron microscopy (TEM) measurement was carried out using FEI Tecnai G2 F20 S-TWIN at 200 kV. The elemental mapping was recorded on a JEM-F200 at the voltage of 200 kV. Proton nuclear magnetic resonance spectroscopy (^{1}H-NMR) was measured on the Bruker AVANCE AV 400MHz facility. Powder X-ray diffraction (PXRD) patterns were recorded on D/MAX-TTRIII (CBO) with Cu Kα radiation (λ = 1.542 Å) operating at 50 kV and 300 mA. Fourier transform infrared (FTIR) spectra were recorded on a Spectrum One in the spectral range of 400−4000 cm^{-1} using the KBr disk method. The Pt contents in the different samples were determined by an inductively coupled plasma mass spectrometer (ICP-MS, Thermo Fisher Scientific). Nuclear magnetic resonance (NMR) was measured on

Bruker AVANCE III HD 400 machine. The circular dichroism (CD) spectrum was recorded on a JASCO-J1500 spectrometer, and an additional integrating sphere detector as well as a solid-sample holder (DRCD-574) are requested when testing solid CMOF samples.
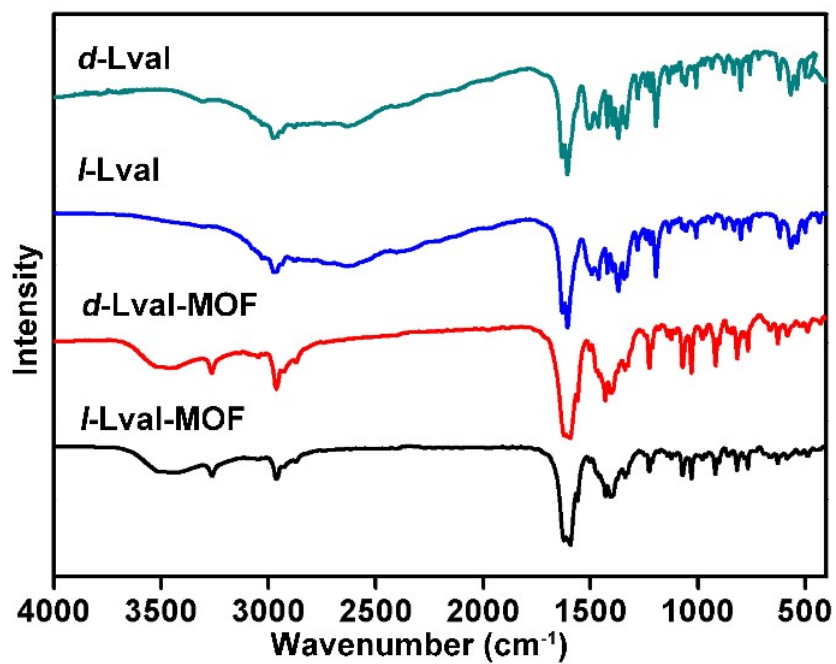
Part S4. Supplemented Figures and Tables.

Figure S1. The IR plots of as-synthesized *l*(*d*)-Lval ligands and corresponding *l*(*d*)-Val-MOFs.
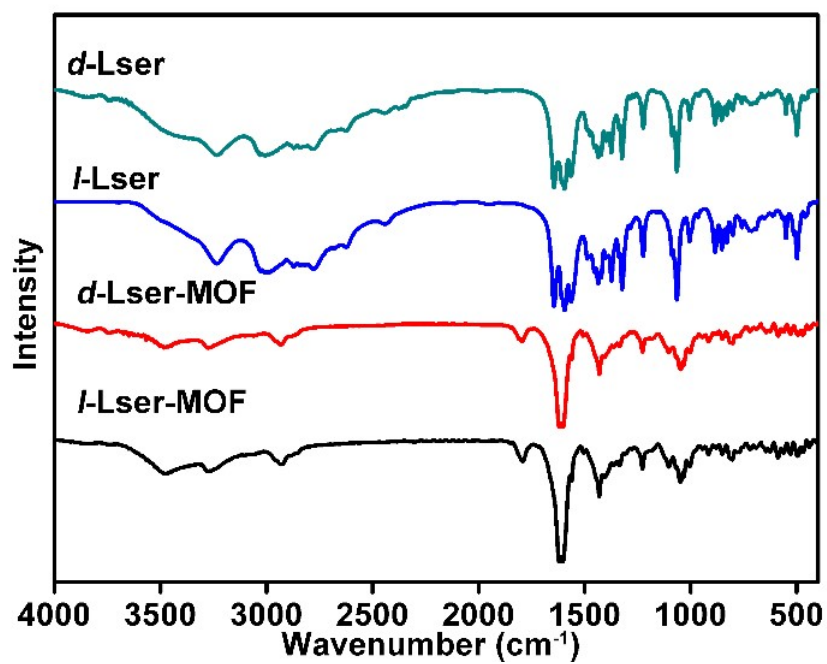
Figure S2. The IR plots of as-synthesized *l*(*d*)-Lser ligands and corresponding *l*(*d*)-Ser-MOFs.
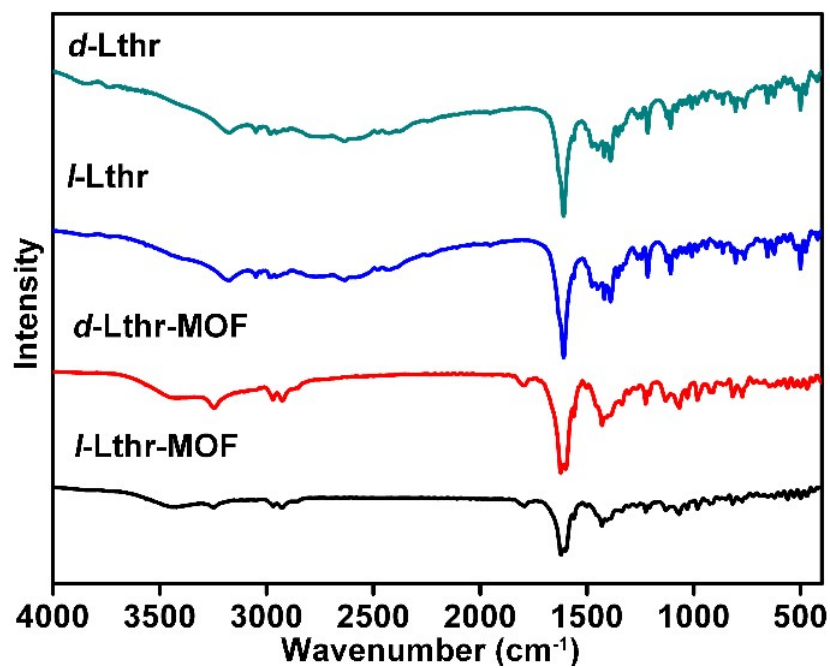
Figure S3. The IR plots of as-synthesized *l*(*d*)-Lthr ligands and corresponding *l*(*d*)-Thr-MOFs.

Table S1 Comparison of the PXRD peak positions of all synthesized CMOFs.

Sample	(1 0 0)	(2 $\bar{1}$ 0)	(2 0 0)	(3 0 0)	(1 0 $\bar{2}$)
Simulated[a]	5.76	9.99	11.54	17.35	17.75
l-Val-MOF	5.76	10.00	11.56	17.36	17.78
d-Val-MOF	5.78	9.98	11.60	17.38	17.76
l-Ser-MOF	5.82	9.98	11.66	17.42	17.84
d-Ser-MOF	5.84	9.98	11.68	17.44	17.86
l-Thr-MOF	5.78	10.00	11.58	17.40	17.84
d-Thr-MOF	5.76	10.00	11.56	17.38	17.84

[a]The simulated data have adopted the reported crystallography information of Val-MOF from the reference.[2]

We have summarized the PXRD peak positions of all CMOFs and compared them with the simulated one. First of all, the five main peak positions of synthesized *l*(*d*)-Val-MOFs are in line with the simulated one, confirming their successful constructions. Moreover, *l*(*d*)-Ser-MOFs and *l*(*d*)-Thr-MOFs also show nearly identical diffraction peak positions to the *l*(*d*)-Val-MOFs also the simulated one. As a result, it is convincible to conclude the isoreticular crystal structures of those CMOFs based on both Figure 1(g) and Table S1.
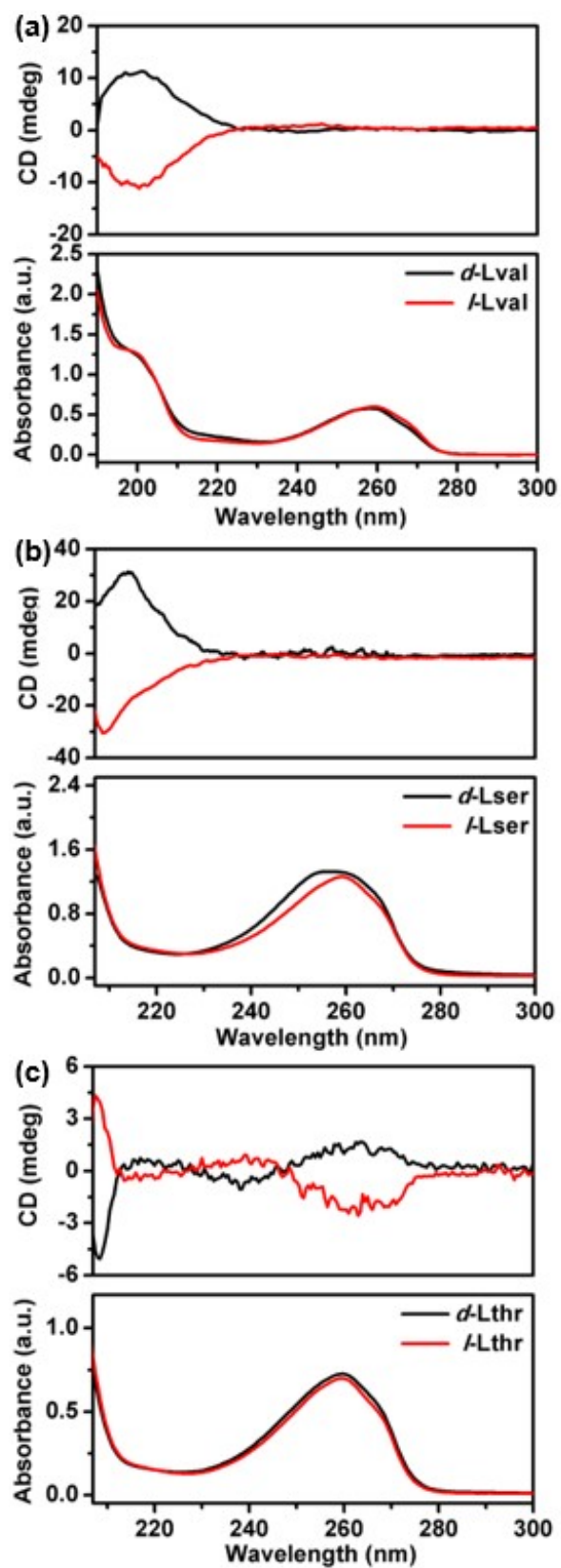
Figure S4. The CD and normal absorption spectra of as-synthesized (a) *l*(*d*)-Lval ligands, (b) *l*(*d*)-Lser ligands and (c) *l*(*d*)-Lthr ligands.

As shown in Figure S4, the absorption peaks centered at 258 nm can be assigned to the extinction of pyridyl ring, also confirming the successful introduction of pyridyl group into corresponding amino acid-derived chiral ligands. More importantly, the mirror-like CD responses offered by each pair of enantiomers also verify their well-maintained chirality.
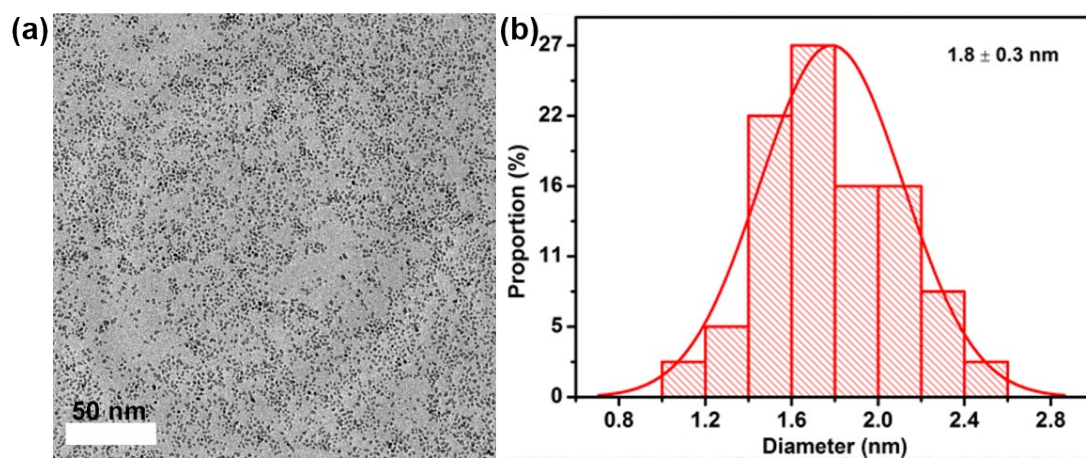
Figure S5. The TEM image of synthesized Pt NPs with an averaged diameter of 1.8 nm.
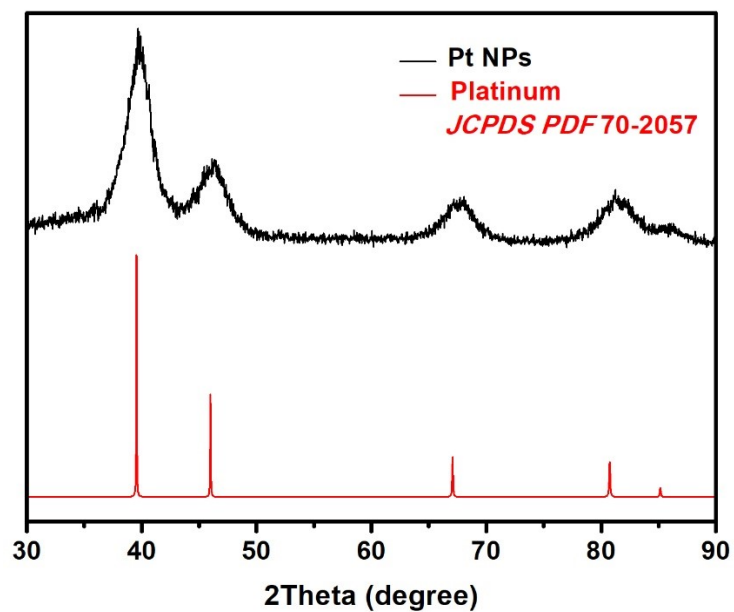
Figure S6. PXRD pattern of the synthesized Pt NPs.

As the pattern shown in Figure S6, the diffraction peaks of synthesized Pt NPs are in line with the face-centered-cubic (*fcc*) standard Pt PDF card (70-2057).
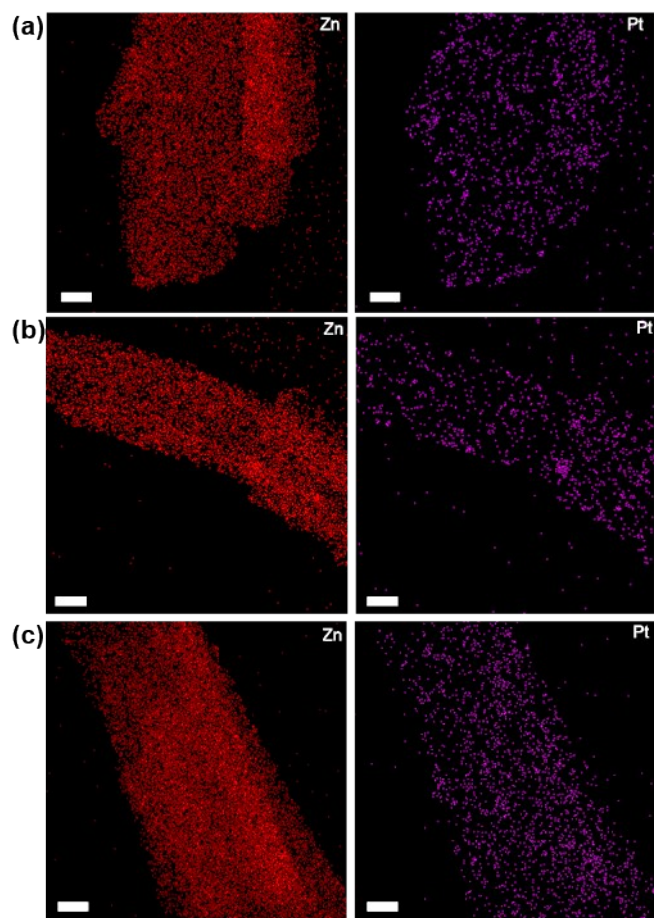
Figure S7. The TEM elemental mapping images of (a) Pt-*l*-Val-MOF, (b) Pt-*l*-Ser-MOF and (c) Pt-*l*-Thr-MOF. The unlabeled scale bars are 50 nm.
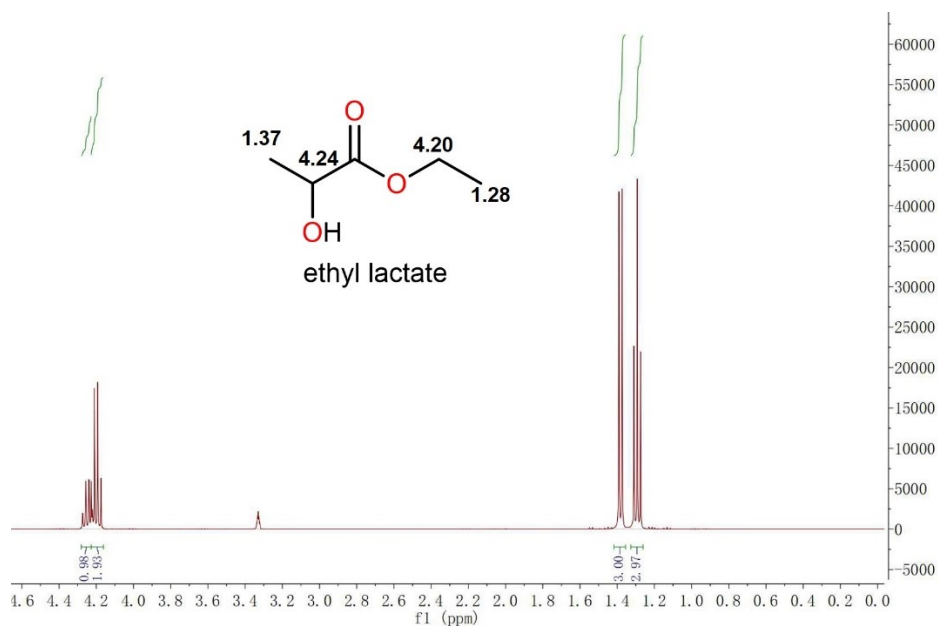
Figure S8. ^{1}H-NMR spectrum of the produced ethyl lactate in CD$_3$OD.

As shown in Figure S8, the product has been unambiguously verified as ethyl lactate [-CH$_3$ (1.28, t), -CH$_3$ (1.37, d), -CH$_2$ (4.20, q), -CH (4.24, q) and no active -OH hydrogen peak observed due to its exchange with CD$_3$OD] with a nearly equimolar conversion.
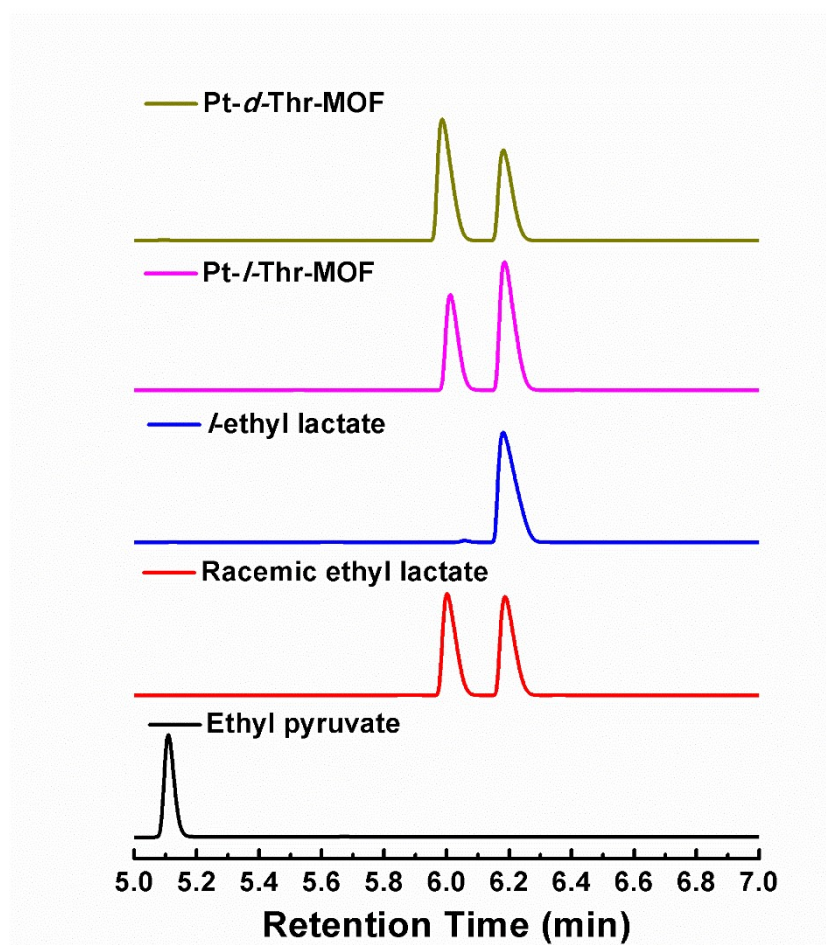
Figure S9. The evaluation of ee value of produced ethyl lactate by chiral GC.

As plots shown in Figure S9, the EP substrate appeared at the retention time of 5.12 min while the racemic ethyl lactate split into two peaks (6.12 min and 6.21 min) with identical integrating peak areas. With the assistance of authorized *l*-ethyl lactate that appeared at 6.21 min, we can easily figure out the biased chiral configuration of catalysis product. As the dark-yellow plot indicated (corresponding to the catalytic performance of Entry 10 in Table 1 of the body part), the Pt-*d*-Thr-MOF enriched the *d*-ethyl lactate product with an ee value of 22.8% based on the integrated peak areas. While the pink plot claimed that the Pt-*l*-Thr-MOF (corresponding to the catalytic performance of Entry 11 in Table 1 of the body part) enriched the *l*-ethyl lactate product with an ee value of 23.9% based on the integrated peak areas. The disappearances of peaks of EP substrate in both case also mean its near equimolar conversion.
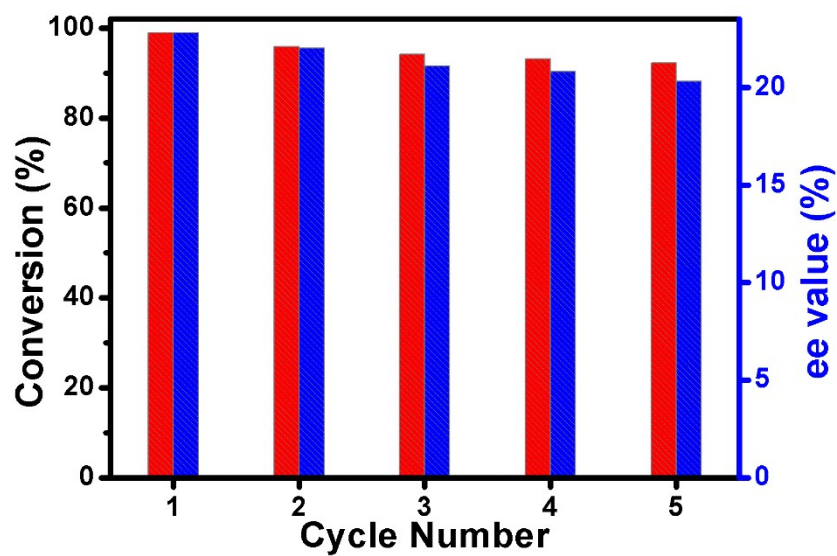
Figure S10. The catalytic recyclability of Pt-*d*-Thr-MOF in the asymmetric hydrogenation of EP.

As shown in Figure S10, Pt-*d*-Thr-MOF can nearly maintain the catalytic performance after 5 catalysis cycles (92.3% in conversion and 20.3% in ee value).
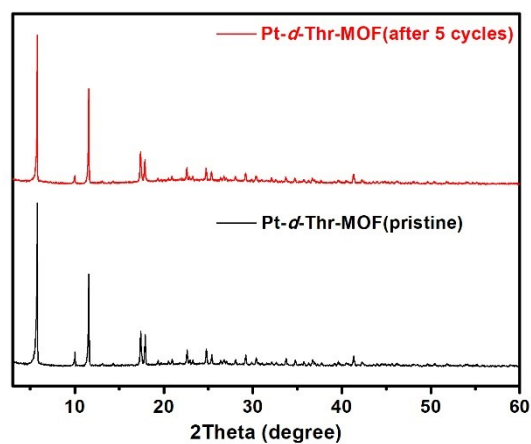
Figure S11. PXRD characterizations of the pristine and recycled Pt-*d*-Thr-MOF asymmetric catalyst.

As shown in Figure S11, the recovered catalyst exhibited a nearly identical PXRD pattern to the pristine one, reflection of the well-retained crystallinity of the Pt-*d*-Thr-MOF asymmetric catalyst.
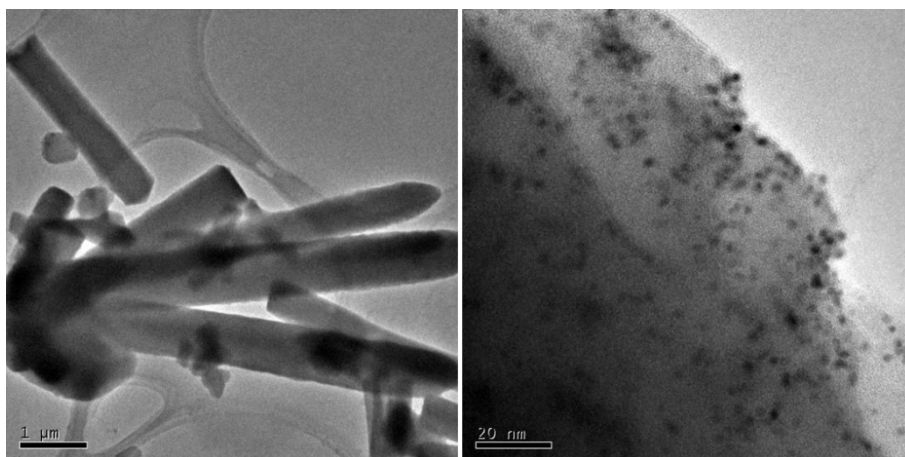
Figure S12. TEM visualization of the recovered Pt-*d*-Thr-MOF asymmetric catalyst.

TEM images also present that Pt NPs are still independently distributed on the surface of *d*-Thr-MOF without obvious aggregations. Which have together confirmed the good recyclability of Pt-*d*-Thr-MOF asymmetric catalyst.

Table S2. The asymmetric catalytic performance comparison with other works.

Catalyst	Substrate	Chiral ligand	Fresh ligands required for recycling	T (ºC)	H$_2$ (bar)	Yield (%)	ee (%)	Ref.
Pt/MIL-101[a]	Ethyl pyruvate	Cinchonidine	Yes	25	40	98.5	44.4	S5
Pt/MIL-101	Ethyl pyruvate	Cinchonine	Yes	25	40	41.8	10.2	S5
Rh NPs	Ethyl pyruvate	Quinine	Yes	20	50	99.7	6.6	S6
Rh NPs	Ethyl pyruvate	Cinchonidine	Yes	20	50	99.5	45.5	S6
Pt/Al$_2$O$_3$	Methyl acetoacetate	Threonine	No	20	20	99	10	S7
Pt/Al$_2$O$_3$	Methyl acetoacetate	Valine	No	20	20	99	20	S7
Pt/Al$_2$O$_3$	Methyl benzoylformate	Proline derivate	Yes	25	10	27	11	S8
Pt/AC[b]	Ethyl pyruvate	Cinchonidine	Yes	20	60	99	61	S9
PVA[c]-Pt/Al$_2$O$_3$	Ethyl pyruvate	Cinchonidine	Yes	25	1	>99	33	S10
PVA-Pt/Al$_2$O$_3$	Ethyl pyruvate	Cinchonidine	Yes	25	50	>99	57	S10
Pt/Al$_2$O$_3$	Acetophenone	Proline	No	20	20	99	15	S11
Pt/Al$_2$O$_3$	Methyl pyruvate	Proline	No	20	20	99	10	S12
Pt-l-Thr-MOF	Ethyl pyruvate	None	No	25	40	99.5	23.9	This work
Pt-d-Thr-MOF	Ethyl pyruvate	None	No	25	40	98.9	22.8	This work

[a]MIL-101 = [Cr$_3$(O)X(bdc)$_3$(H$_2$O)$_2$]·nH$_2$O(bdc=benzene-1,4- dicarboxylate, X=(OH or F)

[b]AC = active carbon, [c]PVA = poly(vinyl alcohol)

As data listed in Table S2, Pt-*l*(*d*)-Thr-MOFs in this work have exhibited excellent conversion efficiency comparable to that reported in some other works, which have been contributed by the large surface area and highly porous nature of *l*(*d*)-Thr-MOF supporters. Moreover, the stereoselectivities reported in this work are higher than amino acid derivates but inferior to the privileged cinchona alkaloid ligands in a few cases based on the data in Table S2. But, the suggested Pt-*l*(*d*)-Thr-MOFs have shown great advantages as novel chiral supporters in the asymmetric catalysis recycling as no additional fresh chiral ligands are required adding into successive catalysis reaction runs. As a return, the expensive ligand cost is savable and also no additional procedures are needed for the separation of the leached chiral ligands as well as the purification of the final chiral product. Which are highly keened for green and sustainable industrial catalysis. More significantly, this work proposed a novel and workable protocol to design and engineer CMOFs at single-chiral site level for targeted applications (e.g., chiral separation, enantioselective sensing and biomedicine) beyond asymmetric catalysis.
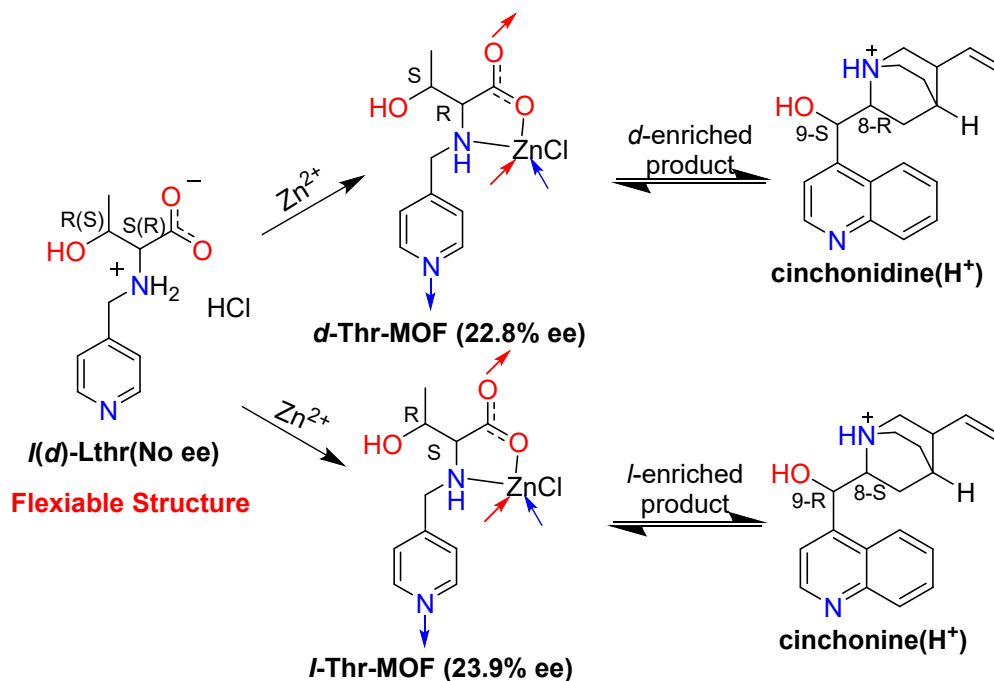
Figure S13. The chiral configuration relationship between catalyst and product.

It is generally accepted that cinchonine/cinchonidine bias the *l*- and *d*-ethyl lactate, respectively.[5, 9, 13] As same as the absolte configurations (8S,9R) of chiral carbon atoms in cinchonine, *l*-Thr-MOF enriched *l*-ethyl lactate product as it also features corresponding (S,R) carbon atoms connecting to amine and hydroxyl groups in sequence. Vice versa, *d*-Thr-MOF is characteristic of (R,S) carbon atoms connecting to amine and hydroxyl groups, respectively, and therefore enriched *d*-ethyl lactate product as same as cinchonidine.

Part S5. References.

[1] Guo, J.; Zhang, Y.; Zhu, Y.; Long, C.; Zhao, M.; He, M.; Zhang, X.; Lv, J.; Han, B.; Tang, Z., *Angew. Chem. Int. Ed.* 2018**, 57**, 6873-6877.

[2] Sahoo, S. C.; Kundu, T.; Banerjee, R., *J. Am. Chem. Soc.* 2011**, 133**, 17950-17958.

[3] Zhao, M.; Yuan, K.; Wang, Y.; Li, G.; Guo, J.; Gu, L.; Hu, W.; Zhao, H.; Tang, Z., *Nature* 2016**, 539**, 76-80.

[4] Neumann, S.; Grotheer, S.; Tielke, J.; Schrader, I.; Quinson, J.; Zana, A.; Oezaslan, M.; Arenz, M.; Kunz, S., *J. Mater. Chem. A* 2017**, 5**, 6140-6145.

[5] Pan, H.; Li, X.; Zhang, D.; Guan, Y.; Wu, P., *J. Mol. Catal. A: Chem.* 2013**, 377**, 108-114.

[6] Jiang, H.-y.; Xu, J.; Sun, B., *Chirality* 2019**, 31**, 818-823.

[7] Šulce, A.; Backenköhler, J.; Schrader, I.; Piane, M. D.; Müller, C.; Wark, A.; Ciacchi, L. C.; Azov, V.; Kunz, S., *Catal. Sci. Technol.* 2018**, 8**, 6062-6075.

[8] Holland, M. C.; Meemken, F.; Baiker, A.; Gilmour, R., *J. Mol. Catal. A: Chem.* 2015**, 396**, 335-345.

[9] Chen, Z.; Guan, Z.; Li, M.; Yang, Q.; Li, C., *Angew. Chem. Int. Ed.* 2011**, 50**, 4913-4917.

[10] Chung, I.; Song, B.; Kim, J.; Yun, Y., *ACS Cata.* 2021**, 11**, 31-42.

[11] Schrader, I.; Warneke, J.; Backenköhler, J.; Kunz, S., *J. Am. Chem. Soc.* 2015**, 137**, 905-912.

[12] Šulce, A.; Mitschke, N.; Azov, V.; Kunz, S., *ChemCatChem* 2019**, 11**, 2732-2742.

[13] Sharma, P.; Sharma, R. K., *New J. Chem.* 2016**, 40**, 9038-9041.